International Symposium on Niobium Microalloyed Sheet Steel for Automotive Application
Edited by S. Hashimoto, S. Jansto, H. Mohrbacher, and F. Siciliano
TMS (The Minerals, Metals & Materials Society), 2006

INTEGRATED PROCESS-METALLURGY MODELLING FOR NIOBIUM MICROALLOYED HOT ROLLED STEELS

A. Perlade, P. Maugis, M. Gouné, T. Iung, D. Grandemange

Arcelor Research, Arcelor Group
Voie Romaine, BP 30320, 57283 Maizières-lès-Metz Cedex, France.

Abstract

The prediction of microstructures and mechanical properties is an important point for the control of steel properties and quality. Numerous models, either physical or more phenomenological, developed by Arcelor R&D laboratories are being assembled in a through-process modeling scheme, to simulate the production process, the thermomechanical history of a steel product, its metallurgical evolution and final properties.

In the case of a niobium microalloyed steel, a model for predicting the precipitation state of Nb as a function of time is used. It describes the full precipitation kinetics from the nucleation stage to the Oswald ripening stage, solving numerically the set of coupled equations for nucleation, growth and coarsening. It gives the volume fraction, mean radius and number of NbC precipitates, and consequently, the niobium and carbon remaining in solid solution.

This precipitation state is of prime importance to control the final mechanical properties of hot-rolled HSLA steels. Other microstructural factors play a key role on the final properties, especially the grain size and the phase fractions that depend on the thermomechanical history of the strip. The physical precipitation model has thus been introduced in an integrated model to predict the microstructure and mechanical properties of hot rolled steel, including the microstructure of C–Mn and C–Mn–Nb steels, the strength, the cooling curve affected by heat evolution due to transformation and the precipitation strengthening.

On-line prediction of microstructure and mechanical properties has been applied to three hot strip mills in Arcelor equipped with advanced process computer systems. One of the main applications of this computer metallurgy is to provide assistance for designing metallurgical routes, since the metallurgical model is a good tool to analyze the different sources of strengthening (grain size, alloying, phase fraction) in relation to chemical compositions and process conditions.

Computing mechanical properties of the strip over the entire strip length is another feature of the on-line system when conventional quality controls are usually only available at the strip head and tail. As an example, this modeling is applied to evaluate the distributions of tensile strengths in strips, which are different between a Nb-microalloyed steel and a non-microalloyed steel.

Introduction

The objective in designing new alloys with the optimum strength/ductility/cost balance for the different components presents a serious challenge to steel manufacturers. Here, the key to success lies in controlling the steel microstructure on the finest possible scale. To do this requires as basic ingredients the development of more accurate thermodynamic and structure/properties models and the coupling of the above to production process models.

Arcelor R&D has thus developed a physical model for predicting mechanical properties of hot rolled strips especially applicable to HSLA C-Mn-Nb steels. Some of the main objectives of this "computer metallurgy" are to provide assistance for designing metallurgical routes, since the metallurgical model is a good tool to analyze the different sources of strengthening (grain size, alloying, phase fraction) in relation to chemical compositions and process conditions. Computing mechanical properties of the strip over the entire strip length is another feature of the on-line system when conventional quality controls are usually only available at the strip head and tail.

Physical Model

The integrated model for predicting microstructural evolution and mechanical properties of hot rolled strips consists of several elemental models, either physical or phenomenological based on more complex models.

In the case of niobium microalloyed steels, the precipitation state is of prime importance to control the final mechanical properties of hot-rolled HSLA steels. Other microstructural factors play a role on the final properties, especially the grain size and the phase fractions that depend on the thermomechanical history of the strip. The influence of niobium on the final mechanical properties is thus taken into account through the:

- Effect on the austenite microstructure after finishing. Since it retards recrystallisation, niobium has a great influence on the predicted effective austenite grain size as a function of the residual strain.
- Effect on the final ferrite grain size,
- Calculation of the precipitation hardening taking into account the thermal evolution of each point in the coil and prediction of the whole tensile curve.

<u>Microstructural evolution during hot rolling and effect on final ferrite grain size</u>

In the reheating furnace, dissolution of precipitates AlN, TiN, Nb(C,N) and solid solution composition are calculated according to thermodynamic equilibrium. Due to the long reheating times, the kinetics effects are reasonably neglected.

During hot rolling, various metallurgical phenomena occur, especially work hardening, dynamic and static recovery and recrystallization of the deformed austenite, precipitation and austenite grain growth. Some complex models have been proposed to describe the metallurgical evolution of austenite during rolling [1], which shows that niobium has a great influence on the final austenite grain size since it retards the recrystallization and increases the residual strain in austenite (Figure 1).

Calculations show that nearly complete recrystallization occurs for grade A, contrary to grade B. In this last case, due to Nb, final austenite is fully deformed and strain is accumulated during the last 5 stands.

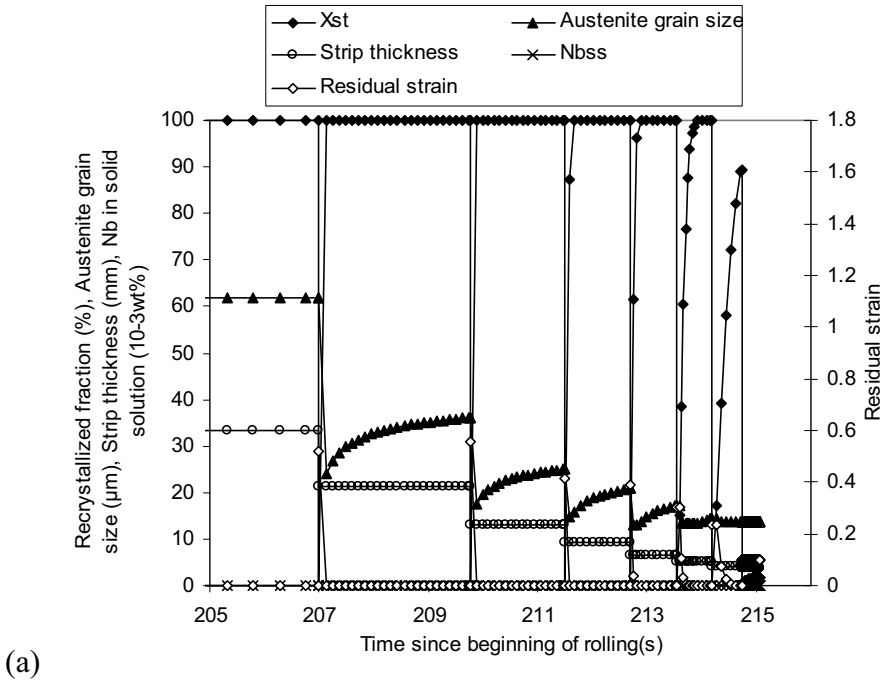

(a)

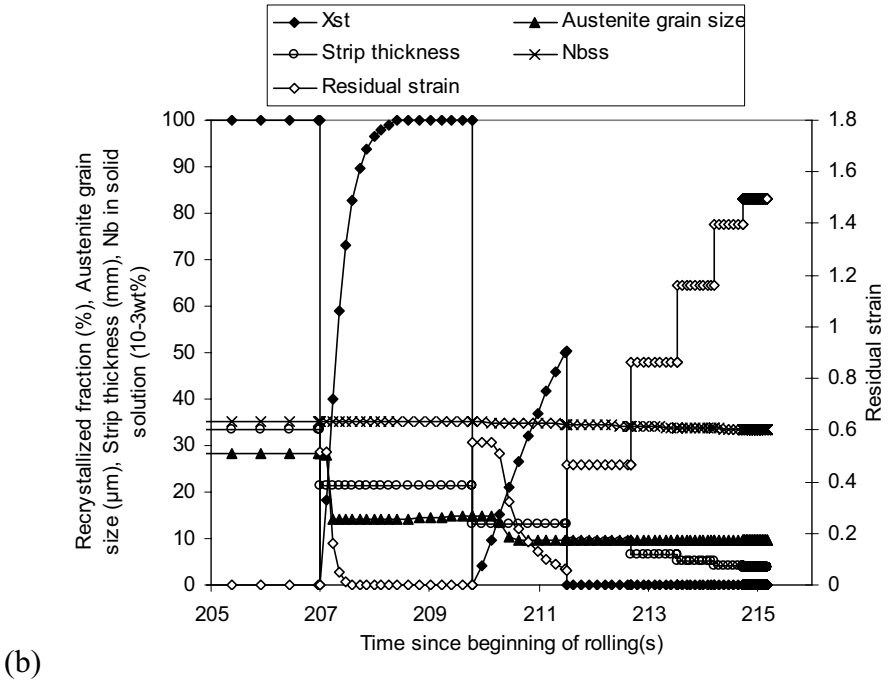

(b)

Figure 1. Evolution of austenite microstructure in the finishing mill according to FAST model for a) Grade A: C75, Mn300 (10^{-3} wt%), b) Grade B: similar to A + 35. 10^{-3} wt%.

According to one of these complete models developed in Arcelor [1], it is found that a much simpler approach can be adopted without significantly affecting the final mechanical properties. An effective austenite grain size at the end of the finishing mill is thus fitted from the results of the complete model as a function of rolling temperature, chemical composition and rolling reduction in the finishing mill (Eq.1). In the case of Nb-microalloyed steels, this effective grain

size is reduced due to a high amount of residual strain, which strongly refines the final ferrite grain size (Eq. 2, 3 and Figure 2).

$$d\gamma = f(\varepsilon_{finishing}, T_{rolling}, \%C, \%Mn) \quad (1)$$

$$d\gamma_{eff} = d\gamma^{\left(1-\frac{C}{B}\cdot\sqrt{\varepsilon_{res}}\right)} \quad (2)$$

$$d\alpha = A \cdot d\gamma_{eff}^{\ B} \cdot V_{ref}^{\ -D} \quad (3)$$

(a)

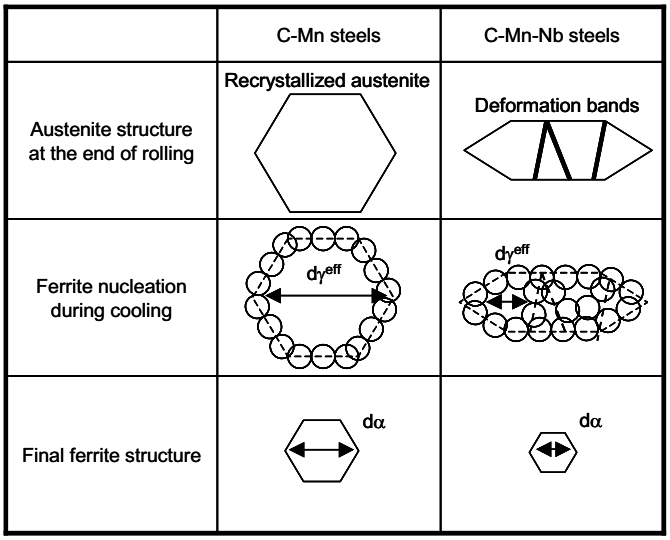

(b)

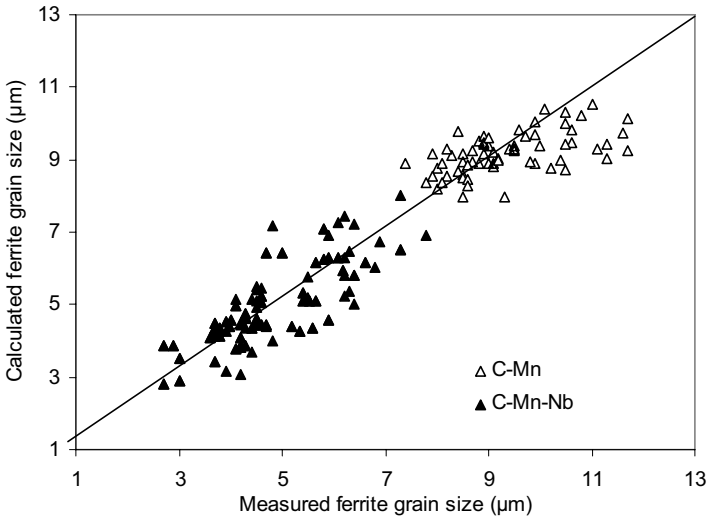

Figure 2. a) The effect of residual strain in the austenite through the effective austenite grain size on final ferrite grain size is schematically described. b) The simplified approach for grain size prediction gives good agreement with experimental measurements.

The thermal evolution and phase transformation on the run-out-table are also taken into account to predict the phase fractions and main transformation temperatures. Models are detailed elsewhere [2].

Precipitation

The MultiPreci model is a class model predicting NbC precipitation kinetics, inspired by previous papers [3, 4] and described in [5, 6, 7]. It is a numerical treatment of the diffusion-limited precipitation kinetics. In the computation algorithm, precipitates having the same radius form a class of particles and evolve at the same rate. The nucleation rate is given by the classical theory and furnishes the number of particles per unit of volume that appear during each time step of the calculation:

$$\frac{dN}{dt} = N_0 Z\beta^* \exp\left(-\frac{\Delta G^*}{kT}\right) \cdot \left[1 - \exp\left(-\frac{t}{\tau}\right)\right] \quad (4)$$

where N is the number of precipitates per unit volume, N_0 the number of nucleation sites, ΔG^* the nucleation barrier, β^* the absorption frequency of a niobium atom, Z the Zeldovitch factor and τ the incubation time.

The growth rate gives the variation of the radius of each particle class during the same time step:

$$\frac{dR}{dt} = \frac{D_{Nb}}{R} \cdot \frac{c^{Nb} - c_i^{Nb}}{c_{pp}^{Nb} \frac{V_{Fe}}{V_{NbC}} - c_i^{Nb}} \quad (5)$$

where R is the radius of each class of particles, D_{Nb} the diffusion coefficient of niobium, c^{Nb} the average atomic fraction of Nb in solid solution, V_{Fe} the volume of an iron atom in ferrite and V_{NbC} the volume of a molecule of NbC. c_i^{Nb} is the atomic fraction of Nb at the particle/matrix interface. The calculation of c_i^{Nb} is based on the local thermodynamic equilibrium and on the flux equality, taking into account the Gibbs-Thomson effect. The formulation of the growth rate is also applicable to dissolution, which allows treating the coarsening stage of precipitation. When applied to precipitation in ferrite, the parameters of the model have been adjusted to $D_{Nb} = 650 cm^2/s \exp(-32475/T)$, the interface energy $\gamma = 0.65$ and a solubility product of $\log_{10}(\%Nb.\%C) = -6637/T + 0.45$.

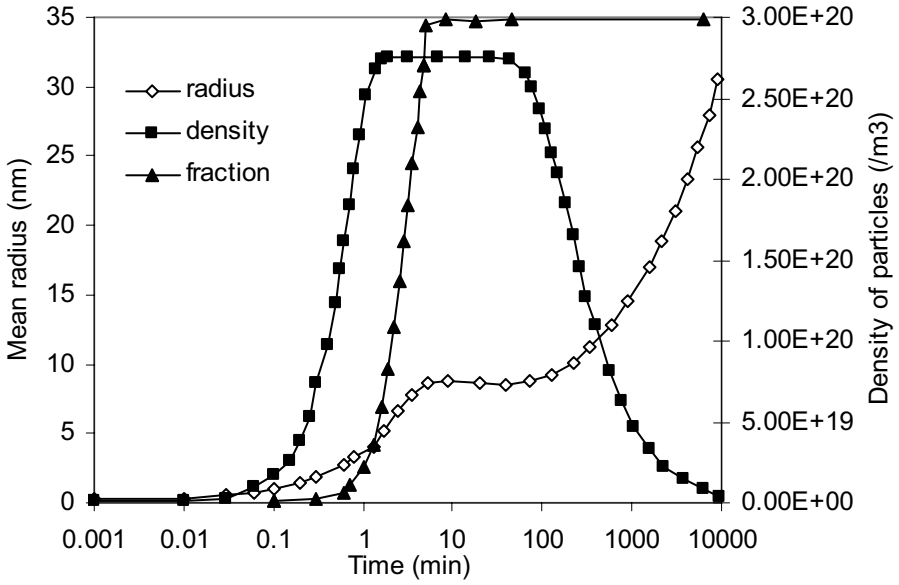

Figure 3. Calculation of time evolution of mean radius, precipitate fraction and density of particles for a steel of composition 105×10^{-3}wt%Nb, 9×10^{-3}wt%C aged at 700°C.

With such a numerical treatment, the model gives the time evolution of the distribution of precipitates in the matrix, from which the mean radius, the density of particles and the precipitated fraction are calculated. As an example, the main results for a steel of composition 105×10^{-3}wt% Nb, 9×10^{-3}wt% C annealed at 700°C are given in Figure 3. The transformation occurs in three stages: nucleation, growth and coarsening that are not fully separated. Carbon and niobium in solid solution decrease continuously accordingly with the increase of the precipitate volume fraction.

Mechanical properties

Ferrite-pearlite microstructure

The whole strengthening curve of the ferrite-pearlite steel is predicted by a physical approach based on the competition between accumulation and annihilation by dynamic recovery of forest dislocations. It implies that ferrite and pearlite flow stresses are related to microstructural features such as ferritic grain size and interlamellar spacing respectively. The flow stresses of each phase can be written as follows:

$$\sigma_1 = \sigma_0 + \frac{\alpha.M.\mu\cdot\sqrt{b}}{\sqrt{d}}\cdot\sqrt{\frac{1-\exp(-f.M.\varepsilon_1)}{f}} \quad \text{for ferrite} \tag{6}$$

$$\sigma_2 = \sigma'_0 + \frac{M.\mu.b}{S} + K\cdot\frac{1-\exp(-g.\varepsilon_2/2)}{g} \quad \text{for pearlite} \tag{7}$$

where α is a constant on the order of 0.4, M is the average Taylor factor (M=3), μ is the shear modulus (80 GPa), b is the Burgers vector ($2{,}5.10^{-10}$m), d is the average ferritic grain size, σ_o is the friction stress, S is the interlamellar spacing of pearlite, K and g are constants respectively equal to 38000 MPa and 70 as identified for fully pearlitic microstructures.

An intermediate mixture law without fitting parameter is used to determine the flow curve of a ferrite-pearlite microstructure [8]:

$$\sigma(\varepsilon) = (1-F)\cdot\sigma_1(\varepsilon_1) + F\cdot\sigma_2(\varepsilon_2) \tag{8}$$

$$\varepsilon = (1-F)\cdot\varepsilon_1 + F\cdot\varepsilon_2 \tag{9}$$

$$\sigma_1(\varepsilon_1)\cdot d\varepsilon_1 = \sigma_2(\varepsilon_2)\cdot d\varepsilon_2 \tag{10}$$

Precipitation strengthening

The hardening effect of niobium carbide precipitates in ferrite differs according to their size, as reviewed for instance by Gladman [9]. The effect of larger precipitates on the stress is taken according to Ashby-Orowan theory for non-coherent precipitates, which are by-passed by dislocations, through the mechanism of Orowan looping [10, 11]:

$$\Delta\sigma_{by-pass} = \beta\frac{\sqrt{f_p}}{d}\cdot\ln\left(\frac{d}{6.125\times10^{-4}}\right) \tag{11}$$

where d is the mean diameter of niobium carbides in μm, fp their volume fraction, related to the proportion of Nb in precipitates in wt% by fp=1.13×10-3 [Nb], and β a constant identified to 17 MPa/μm [2].

Smaller coherent precipitates are sheared by dislocations. The detail of the strengthening mechanism is not known (chemical, modulus or coherency hardening) but, whatever the origin of the critical shearing stress, the hardening contribution to shearing can be correctly described by a law of the form [12]:

$$\Delta\sigma_{shearing} = C \cdot \sqrt{f_p \cdot d} \tag{12}$$

where C is a constant. For each particle radius, the active strengthening mechanism is that corresponding to the smallest of the two values $\Delta\sigma_{by\text{-}pass}$ and $\Delta\sigma_{shearing}$. These values are equal for a critical radius below, which the mechanism changes from looping to shearing (Figure 4a).

When coupling the precipitation model to this mechanical property model, it is shown that the resulting strengthening peak height depends linearly with the Nb content and only very slightly with the C content (Figure 4b). The position of the strengthening peak depends on the critical radius of the precipitate, practically correlated to the thermal path.

According to these results, a simpler approach due to Militzer [13] was used to describe on-line the strengthening curve, which assumes a phenomenological law fitted on both calculation and experimental data (Figure 5).

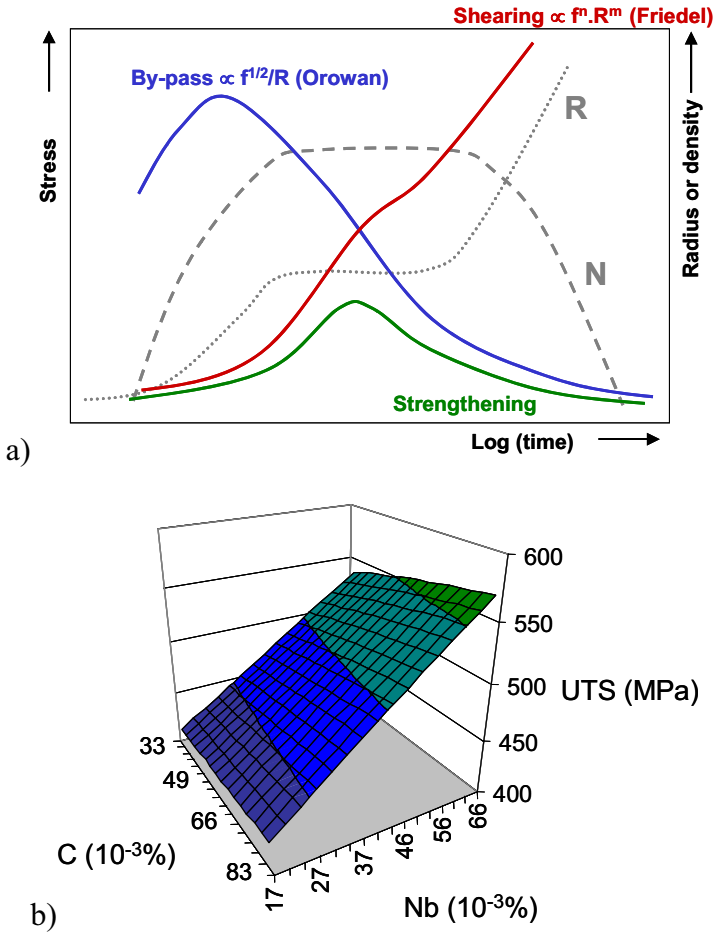

Figure 4. a) Schematic view of the precipitation strengthening curve as a function of isothermal soaking time due to the mechanism changes from looping to shearing when the mean precipitate radius increases. b) Calculations according to the multi-preci model show a linear dependency of the strengthening peak height with Nb content, while C content has nearly no effect.

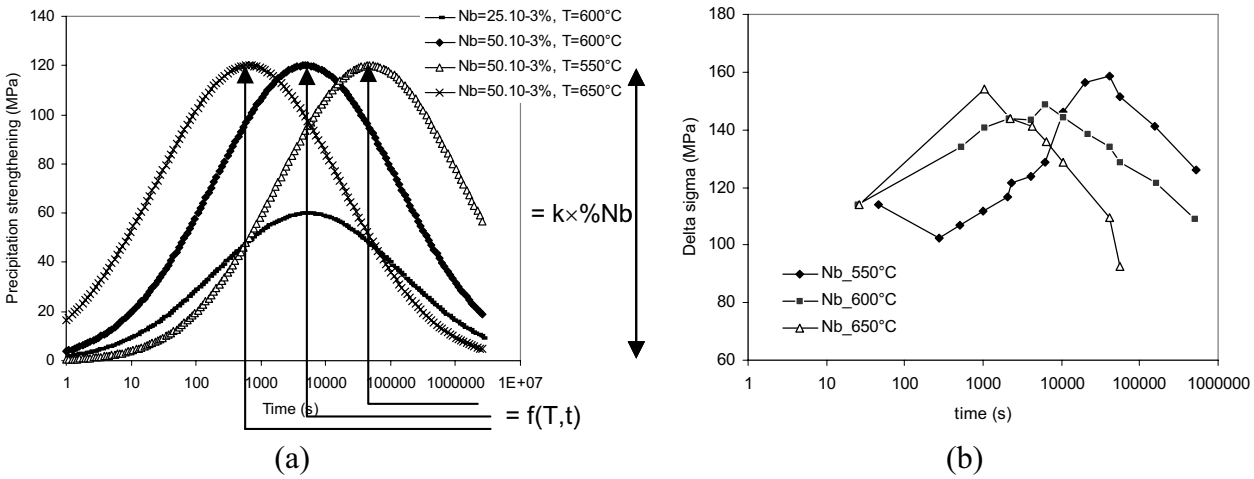

Figure 5. Precipitation strengthening curve according to Militzer approach [13]: the position of the peak, which strongly depends on the thermal path is fitted on experimental isothermal holding (due to Militzer also [13]); the height of the peak is fitted according to results from Multi-preci model shown in Figure 4b.

Coupling with coil cooling

The thermal evolution of each point in the coil is obtained by a linear interpolation from ten typical thermal profiles (from head to tail of the strip) derived from a more complex 2D model [15] (Figure 6). Depending on the position in the coil, various microstructural evolutions are predicted: (i) the softening of pearlite due to globalization [14], (ii) the strengthening due to NbC, TiC and VC precipitation according to Militzer approach [13] and (iii) the nitrogen content in solid solution after TiN, BN and/or AlN precipitation.

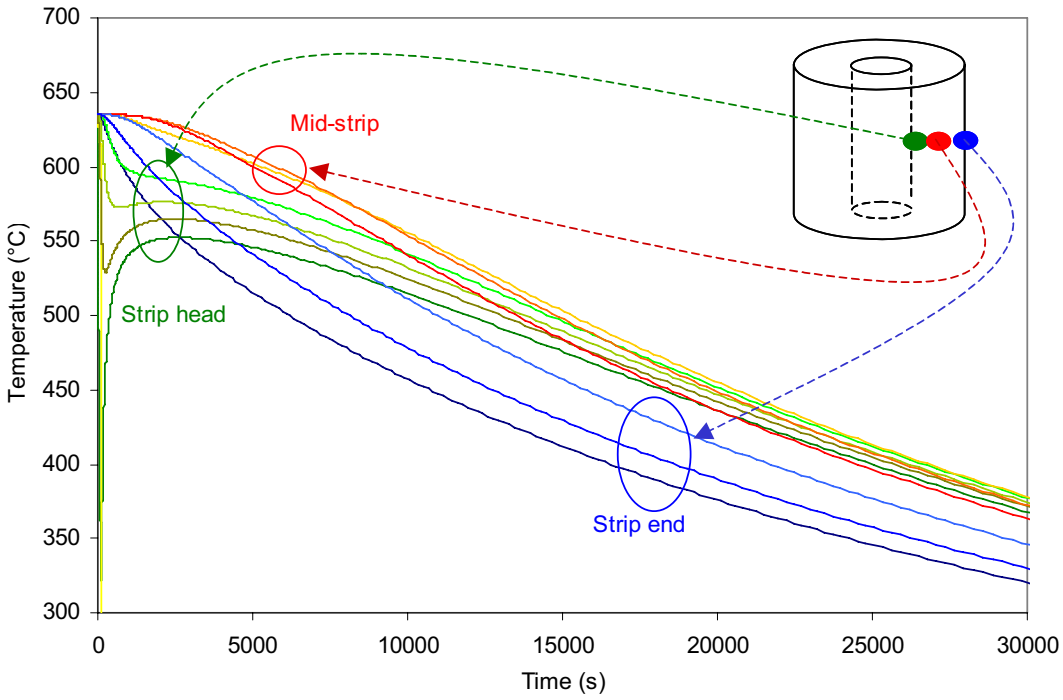

Figure 6. Thermal evolutions at ten different positions in the coil according to a 2-dimension thermal model of the coil, characterised by an imperfect thermal contact between the wraps [15].

Applications

On-line prediction of microstructure and mechanical properties has been applied to three hot strip mills in Arcelor equipped with advanced process computer systems. In each case, the accuracy of the physical model is verified on industrial databases by comparing calculated and measured mechanical properties. The Figure 7 shows a good agreement between the calculated and measured ultimate tensile strengths on Carlam HSM for a wide range of quality grades (C-Mn, HSLA and drawing hot rolled strips).

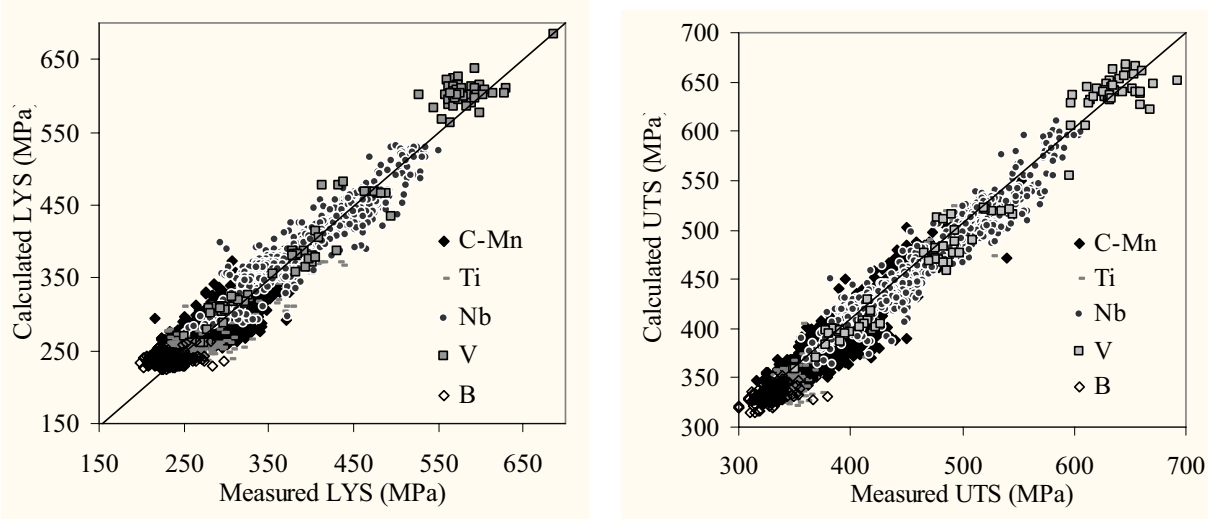

Figure 7: Prediction of the lower yield strength and of the ultimate tensile strength by TACSI for C-Mn, HSLA and drawing hot rolled strips. The accuracy around 13MPa for UTS is very satisfactory.

One of the main applications of this computer metallurgy is to give help for designing metallurgical routes, since the metallurgical model is a good tool to analyze the different sources of strengthening (grain size, alloying, phase fraction) in relation to chemical compositions and process conditions. One example is given in Table I where two grades presenting the same measured UTS are compared to modeling.

Table I: In the case of C-Mn steel (grade A), the UTS target of 470MPa is obtained due to the high C content inducing a high amount of pearlite (21%). On the contrary, in the case of C-Mn-Nb steel, the effect of Nb on precipitation strengthening (55MPa) and on ferrite refinement (4µm instead of 7.7µm) enables a decrease in C content down to 53 x 10^{-3}% (only 5% pearlite).

	C	Mn	Si	Al	Cr	Nb	N	$T_{reheating}$	Thickness	$T_{end\ rolling}$	$T_{coiling}$	YS	LYS	UTS	Ar_3
Units	10^{-3} wt%							°C	mm	°C	°C	MPa	MPa	MPa	°C
Grade A	159	371	12	32	14	0	5	1189	2.3	868	627		355	475	730
Grade B	53	334	13	35	21	25	3	1201	2.0	889	562	422		461	750

	Ar_3	dα	λ	fp	UTS	YS	Precipitation strengthening
Units	°C	µm	Nm	-	MPa	MPa	MPa
Grade A	730	7.7	155	0.21	464	333	0
Grade B	750	4	150	0.05	462	427	55

Computing mechanical properties of the strip over the entire strip length is another feature of the on-line system when conventional quality controls are usually only available at the strip head and tail. As an example, this modeling is applied to evaluate the distributions of tensile strengths in strips for both grades A and B of Table I (Figure 1).

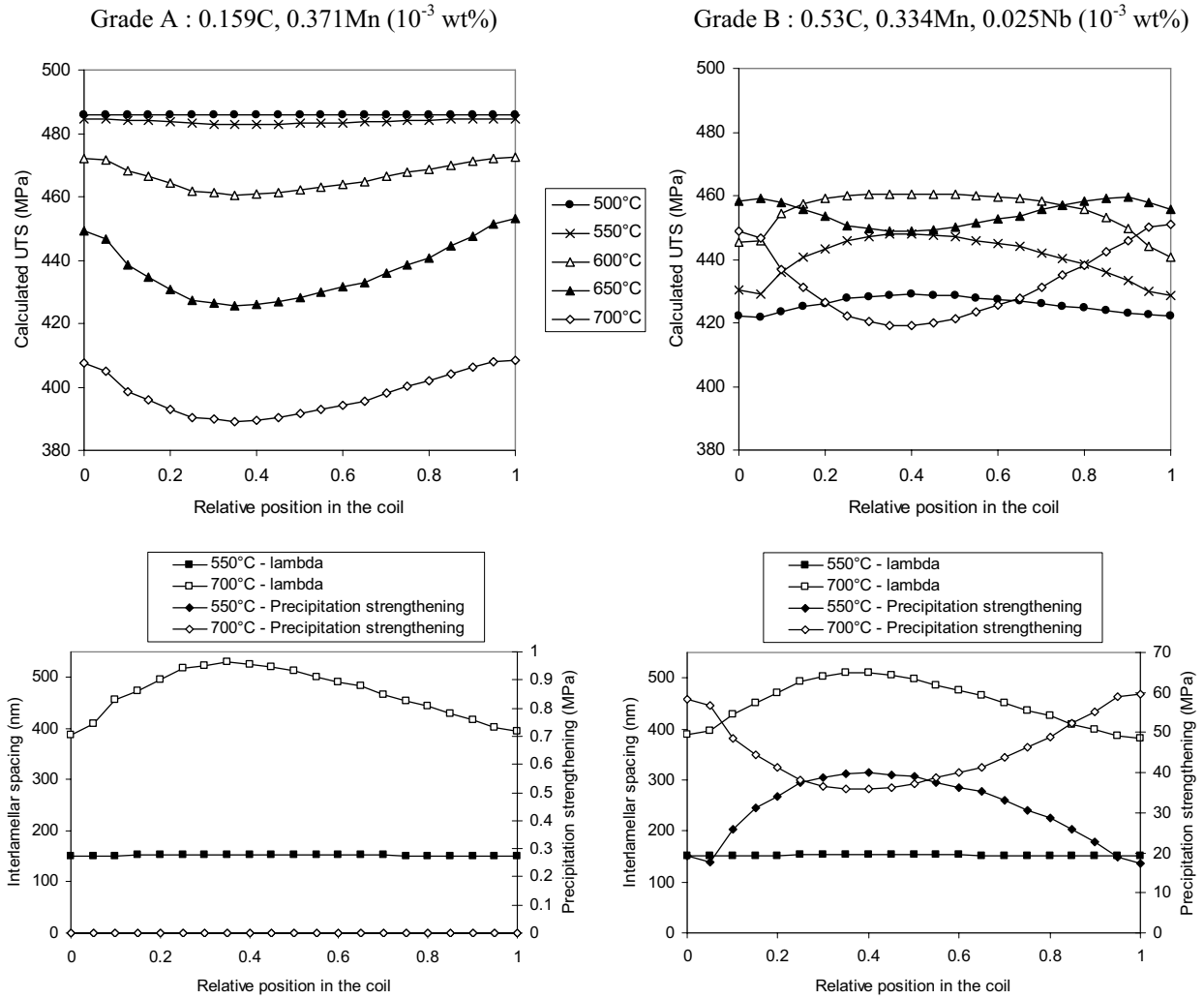

Figure 8: a) The profile of ultimate tensile strengths over the entire strip length strongly depends on the chemistry and on the coiling temperature. b) Modelling enables to visualise the various sources of strengthening and heterogeneity through the coil: precipitation strengthening for microalloyed steels, pearlite softening for "high pearlite" containing grades, described as an increase of interlamellar spacing λ.

C-Mn ferrite-pearlite steels (Example Grade A in Figure 8) are strengthened due to pearlite that softens for long thermal treatment at high temperature: UTS values are thus globally lower as the coiling temperature increases. Some gradients are also observed along the strip length and the decrease in UTS can be as high as 20 to 30 MPa in the middle of the strip.

The UTS profile for Nb-microalloyed steels (Example Grade B in Figure 8) results from a combination of precipitation strengthening and pearlite softening and thus depends on the coiling temperature. At low coiling temperature where precipitation kinetics is slow (Example 550°C in Figure 8), the precipitation strengthening is the highest in the middle of the coil, whereas the interlamellar spacing is nearly not affected: The resulting UTS is thus the highest in the middle of the coil. At higher coiling temperature where precipitation kinetics is fast enough to enable precipitate coarsening (Example 700°C in Figure 8), both low precipitation strengthening and large interlamellar spacing induce a UTS decrease in the middle of the coil.

In this case, modeling can thus be used to determine the optimum coiling temperature to obtain the highest UTS value with reference to the steel chemistry. It might also be used to optimize the

coiling temperature profile industrially applied over the strip length in order to minimize the heterogeneity while maintaining for each point of the strip the optimum strengthening.

Conclusions

Arcelor is developing different models for the description of steel metallurgy and the production process, based on physical descriptions of the phenomena, as far as possible. Some of these models have been applied to the case of cooling of coils at the exit of a hot strip mill, in order to evaluate the heterogeneities of temperature evolution in the product and their effect on mechanical properties through variations of precipitated fraction and precipitate size in a niobium microalloyed steel. By this way, variations obtained in industrial conditions are explained. The general accuracy of this simulation is satisfactory.

A major interest of this integrated process-metallurgy modeling is its use for predictive purposes, like studies of sensitivity to process or composition modifications. Another one, due to its fine level of description, is to make available information on microstructural characteristics, which often cannot be obtained experimentally, like for instance precipitation kinetics in precise locations in the product. Likewise, the information obtained on mechanical properties is the complete behavior law, from which the tensile curve can be deduced, rather than only specific values like tensile strength or uniform elongation.

References

1. P. Choquet, P. Fabrègue, J. Guisti, B. Chamont, J.N. Pezant, F. Blanchet, « Modelling of forces, structure and final properties during the hot rolling process of the hot strip mill », Mathematical modelling of hot rolling of steel, August 26-29, 1990, Hamilton, Ontario, Canada.
2. Perlade, D. Grandemange, T. Iung, “Application of microstructural modelling for quality control and process improvement in hot rolled steels” TMP 2004.
3. J.S. Langer, A.J. Schwartz, Physical Review A, Vol. 21, 1980, p. 948.
4. R. Kampmann, R. Wagner, in Atomic Transport and defects in metals by neutron scattering, Berlin, Springer Verlag, 1986, 73–77.
5. D. Gendt et al., “Modelling of niobium carbide precipitation in steel”, Conf. COM2000, Ottawa, Canada, 30-23 Aug. 2000.
6. P. Maugis, D. Gendt, S. Lanteri, and P. Barges, "Modeling of niobium carbide precipitation in steel." Defect and Diffusion Forum 194-199, 1767 (2001).
7. P. Maugis, M. Gouné, P. Barges, D. Dougnac, D. Ravaine, M. Lamberigts, T. Siwecki, and Y. Bi, "A model for niobium carbonitride precipitation in ferrite." Materials Science Forum 426-432 (4), 1313 (2003).
8. O. Bouaziz, P. Buessler, “Mechanical behavior of multiphase materials: an intermediate mixture law without fitting parameter », Revue de Métallurgie, No. 1 (January 2002), p71
9. T. Gladman, “Precipitation hardening in metals”, Materials Science and Technology, Jan.1999, vol. 15, pp. 30-36.
10. E. Orowan, “Internal stress in metals and alloys”, The Institute of Materials, London, UK, 1948, p. 451.

11. M.F. Ashby, “Oxide dispersion strengthening”, (ed. G.S. Ansell et al.), Gordon and Breach, New York, NY, 1958, p. 143.
12. H.F. Shercliff and M.F. Ashby, “A process model for age hardening of aluminum alloys”, Acta Mat. Vol. 38, No. 10, (1990), p.1789-1812.
13. M. Militzer, E. B. Hawbolt, T.R. Meadocroft, “microstructural model for hot strip rolling of high-strength low-alloy steels”, Metall. And Mat. Trans., 31A, April 2000, 1247-1259.
14. R. Marder, B.L. Bramfitt, “Effect of continuous cooling on the morphology and kinetics of pearlite”, Metallurgical Transactions, Vol. 6A, November 1975, 2009-2014.
15. P. Buessler, P. Maugis, O. Bouaziz, “Integrated process-metallurgy Modeling: example of precipitation during coil cooling”, 44th Mechanical Working and Steel Processing and 8th International Rolling Conference", Orlando, Sept. 2002.